The Energy Transfer and Utilization Mechanisms of Dual-EML Blue OLEDs

Fang Wang, Weimin Ning, Fengping Hu, Ming-Chou Wu

***Wuhan China Star Optoelectronics Semiconductor Display Technology Co., Ltd., Wuhan, China**

Abstract

In current commercializing OLED panels， blue devices still mainly utilize traditional fluorescent emission mechanisms due to the shorter lifetime and low color purity of blue PH-OLEDs and TADF-OLEDs. Despite the internal quantum efficiency (IQE) can be achieved 62.5% by using commercial blue host materials with Triplet-Triplet Fusion (TTF) characteristics, the external quantum efficiency (EQE) of blue fluorescent devices doesn't look respectable on account of incomplete utilization of triplet excitons, such as aggregation-caused quenching (ACQ) and triplet-polaron quenching (TPQ). In recent years, the dual-EML blue devices were developed to improve efficiencies of fluorescence OLEDs. However, the energy transfer and utilization mechanisms are still unclear understanding. To accelerating the commercialization of Dual-EML blue devices, our team present a novel device structure system to analysis the different energy utilization mechanisms between EML1 and EML2. The blue device exhibits high efficiency~300 BI and great improvement of lifetime ~80%, and providing valuable insights in both selecting well-matched BH materials and optimizing device structure.

Author Keywords

OLEDs, Dual-EML, blue light emitting diodes, TTF, TPQ, energy transfer.

1. Introduction

Organic light-emitting diodes (OLEDs) have been established as one of the most promising candidates for human eye-friendly, energy-saving as well as flat-display panels because of its favorable properties such as fabrication on flexible substrates and large-area emission[1], [2], [3]. Blue phosphorescent and thermally activated delayed fluorescent organic light-emitting diodes (PH-OLEDs and TADF-OLEDs), achieving nearly 100% internal quantum efficiency, however, the operational lifetime of both blue PH-OLEDs and TADF-OLEDs remains insufficiently short, hinder their practical use in flat-panel displays.

Blue fluorescent OLEDs have been mass-produced successfully with a Triplet-Triplet Fusion (TTF) typed host material. However, the fluorescent blue dopant can only utilize singlet excitons which proportion is 25%, thus the theoretical internal quantum efficiency is limited to 62.5%. For commercializing OLED panels, the development of blue devices has mainly focused on increasing external quantum efficiency (EQE), reducing the power consumption, and enhancing the operational lifetime, thus the efficiency under high brightness are especially important to reduce the power consumption in flat-panel displays[4], [5]. Generally, blue OLEDs suffer from serious energy consumption due to triplet–triplet annihilation (TTA) and triplet-polaron quenching (TPQ), especially in high driving voltage at charge recombination zone[6], [7].

In 2022，IK reported a paper to solve these problems, and put forward a new concept which consists of two emitting layers called bilayer-EML[8]. The blue host (BH) material in the first emission layer (EML1 : near the anode side) needs to have a higher triplet energy (T+) than BH material in the second emission layer (EML2 : near the cathode side) to make sure sufficient energy transfer which separate recombination zone and TTF zone, and expect to reach both higher EQE and lifetime. Unfortunately, we have fabricated an blue device with reference to this concept, but the performance has not been improved.

In this work, in order to clarify the energy transfer and utilization mechanisms of Dual-EML blue devices, we chose some BH materials with different characteristics and present a novel device structure analysis system to further improve the device efficiency and lifetime, and give a guidance to accelerating the commercialization progress of Dual-EML blue devices. Finally, the novel dual-EML blue device with well-matched BH materials and novel device structure realized a high blue index of 292 and a significant increase of lifetime near 80%.

2. RESULTS AND DISCUSSION

2-1 Characteristics of BH in Dual-EML blue device

In order to verify the material matching principle of Dual-EML, BH1-A, BH1-B and BH1-C have been chosen. The HOMO levels and triplet energies exhibited obviously different with each other (Table 1), and the BH2 was selected as a reference compound which was used to prepare single-EML device.

Table 1. HOMO, LUMO, S_1 and T_1 levels of BHs.

Code	HOMO (eV)	LUMO (eV)	S_1 (eV)	T_1 (eV)
BH1-A	5.88	2.82	3.07	1.95
BH1-B	6.00	3.10	3.08	1.98
BH1-C	5.90	2.91	3.08	1.85
BH2	5.92	2.93	3.05	1.78

To investigate the carrier-transporting characters of BH1-A, BH1-B, BH1-C and BH2, single-carrier devices were fabricated, and their current density–voltage curves are shown in Figure 1. The hole-only devices have structure of indium tin oxide (ITO) / HT:PD (10nm 3%) / HTL (125 nm) / B-Prime (5nm) / BH (20 nm) / HATCN (10nm) / Mg : Ag (2:20). The HATCN/Cathode interfaces was designed to prevent electron-injection from the cathode due to a large electron barrier. These single carrier devices exhibited different hole transporting abilities, BH1-A exhibited comparable hole currents with BH2 at a given voltage, significantly higher than BH1-B and BH1-C, which also has similar HOMO level and the same hole injection efficiency with BH2.

ISSN 0097-996X/25/5603-2296-$1.00 © 2025

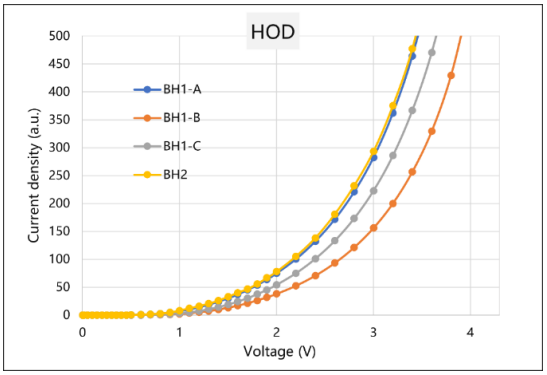

Figure 1. Current density versus voltage curves for the hole-only devices of BH1-A, BH1-B, BH1-C and BH2

In order to study the influence of material characteristics to Dual-EML device performances, bottom blue devices were fabricated. Each Dual-EML blue device (B1-B3) has a typical structure of ITO / HIL (10 nm, 3%) / HTL (125nm) /B-prime (5nm) / BH1-X : BD(5 nm , 2%) / BH2 : BD(15nm : 2%) / HBL(5nm) / ETL : LiQ (30nm, 50%) / Yb(1nm) / Ag(100nm) with BH1-A, BH1-B and BH1-C respectively. The single-EML blue device B4 was also fabricated using the reference compound BH2 for comparison.

The bottom device performance was showed in Table 2. Both B1 and B3 were not observed EQE improvement, and B2 exhibited the best performance (Figure 2) in both EQE (111%) and lifetime (160%) , which was fabricated with BH1-B that possesses the highest T_1 and the lowest hole transporting ability among these three analogs. Despite the T_1 of BH1-A was similar with BH1-B, BH1-B has deeper HOMO and slower hole transport capability than BH1-A, which ensured recombination occurring in the layer with higher triplet energy host (EML1 on the anode side) . On the other hand, even though the hole mobility of BH1-C is slower than BH1-A, its T_1 is significantly lower than both BH1-A and BH1-B. The triplet energy from EML1 cannot transport to EML2 efficiently, thus TTF region was not separate from the recombination zone successfully, and the lack of hole brings lifetime loss.

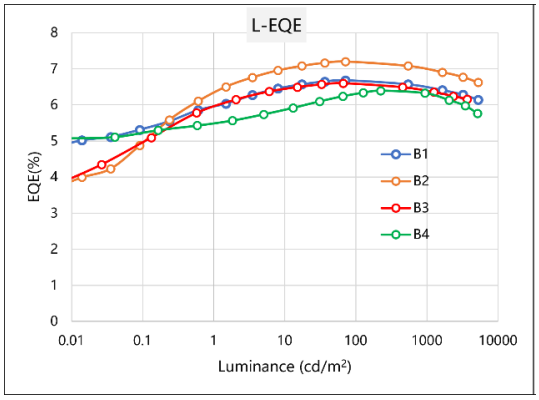

Figure 2. Luminance Vs. EQE curves of B1~B4

Table 2. Electroluminescence characteristics of the bottom blue devices.

Device	Op.V (V)	EQE (%)	LT97@J30
B1	3.24	6.65 (103%)	195 (117%)
B2	3.35	7.35 (111%)	266 (160%)
B3	3.34	6.75 (101%)	135 (81%)
B4	3.21	6.62 (100%)	166 (100%)

As a result, to disperse excitons within the EML, the blue host at EML1 must has a higher triplet energy than the blue host at EML2, and the T_1 gap needs to lager than 0.15eV to make sure energy transfer and separate TTF region from the recombination zone. Last but not least, BH1 needs a slower hole mobility than the blue host in EML2, which ensure the recombination occurs in EML1.

2-2 Novel Dual-EML device structure analysis system

In order to further investigate the method of optimizing device structure to further improve device performance from the perspective of optimizing device structure, dual EML structures with different doping area were fabricated to explore the energy transfer principle so that we can design more efficient energy utilization device structure. As shown in the Figure 3, the 200Å EML were divided into four equal parts with different doping region, and the Dual-EML analysis system was be designed in Table 3.

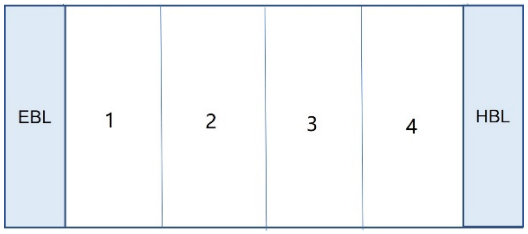

Figure 3. EML partition diagram of dual-EML analysis system

Table 3. Doping method of Dual-EML analysis system.

Device	Doping area			
	1 (50Å)	2 (50Å)	3 (50Å)	4 (50Å)
B5	BH1+BD	BH2+BD	BH2+BD	BH2+BD
B6	BH1+BD	BH2+BD	BH2+BD	**BH2**
B7	BH1+BD	BH2+BD	**BH2**	**BH2**
B8	BH1+BD	**BH2**	BH2+BD	**BH2**

The different performance demonstrated in Table 4. The device efficiency and lifetime of B6 is still much higher than the single EML devices mentioned earlier in the article, indicated that the dopants on the HBL side does not play a decisive role in the efficiency and lifetime upgradation of dual EMLs, which is consistent with our understanding that the exciton recombination region of blue light devices is closer to the EBL side. Significantly, the deficiency of dopants in this region lead to a deterioration in both efficiency and lifetime, which might be caused by the accumulation of triplet excitons in EML2, similar to the excessive concentration of triplet excitons in single EML devices.

It is exciting that B8 presented both higher EQE and lifetime. It is noteworthy that compared with B5-B7, B8 possess a region without dopants between EML1 and EML2. Such device setup can avoid the energy transfer pathway through the high-energy S_1 from EML1 to EML2, which would lead to not only the degradation of interface but also the reduction of exciton concentration in EML2.

On the other hand, by setting BD free buffer zones with lower T_1 host materials can quickly transfer excess excitons in EML1 to EML2, so that device efficiency and lifetime can be improved simultaneously,

Table 4. Electroluminescence characteristics of Dual-EML analysis system.

Device	Vop J10 (V)	EQE J10 (%)	LT97 J30 (hrs)	EL_{peak} (nm)	FWHM (nm)
B5	3.34	7.35	278	462	22
B6	3.34	7.30	249	462	22
B7	3.35	7.11	210	462	22
B8	3.35	7.50	276	462	22

2-3 Application to top emission device

In order to clarify the method of material selection and the Dual-EML analysis system, top emission devices with structure of ITO / HIL (10 nm, 3%) / HTL (125nm) /B-prime (5nm) / EML1 (5 nm , 2%) / EML2 (15nm : 2%) / HBL(5nm) / ETL : LiQ (30nm, 50%) / Yb(1nm) / Mg : Ag(1:10) / CPL were be fabricated. As shown in Figure 4 and Table 5, the highest efficiency and optimal lifetime in devices were achieved by the devices with dual buffer settings. Finally, through the optimization of device structure and optical microcavities, blue devices reached up to a 33% efficiency improvement with BI of 292, and a 80% lifetime improvement, compared with the referred blue fluorescent devices.

Table 5. Electroluminescence characteristics of Dual-EML analysis system.

Device	Vop J10 (V)	BI J10 (CE/CIEy)		LT97 J30 (hrs)	
Ref	3.18	220	100%	115	100%
A’	3.29	284	129%	200	178%
B’	3.29	281	128%	174	148%
C’	3.29	279	127%	170	148%
D’	3.29	292	133%	206	180%

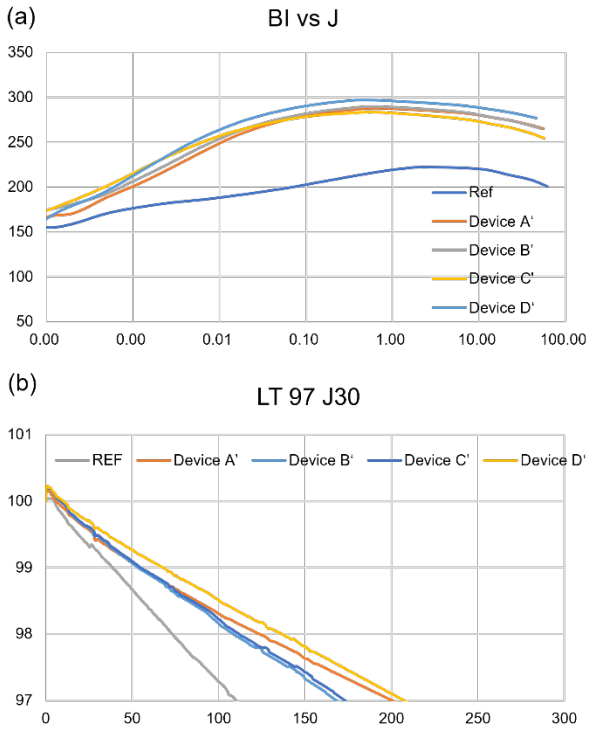

Figure 4. (a) BI vs current density of top-emitting devices (b) Device lifetime curves of top-emitting devices at the current density of 30 mA/cm^2.

3. Conclusion

In summary, we investigated the exciton utilization and energy transfer mechanism in Dual-EML blue devices from the perspectives of materials and devices in this paper. On the one hand, the T_1 of the blue host at EML1 must 0.15eV higher than the triplet energy of BH2 at EML2, and BH1 needs a slower hole mobility than the blue host in EML2, which ensure the recombination occurs in EML1. On the other hand, triplet exciton buffer zone were found to be helpful for the further improvement of device efficiency with the maintained device lifetime. Ultimately, through the material combination and device optimization, we fabricated blue devices with a 33% efficiency improvement and a 80% lifetime improvement, compared with the referred blue fluorescent devices. The highest top-emission device efficiency reached up to 292 with LT97 J30 of 206 hours. Besides, we believe that through the more refined structural adjustments and material matching, the performance of blue devices with dual-EML could be further improved.

4. References

1. L. Zhang, Y. Zhang, Y. Hu, X. Shi, et al. ACS Applied Materials & Interfaces. 2016, 8, 16186;
2. J. Lee, S. Cheng, S. Yoo, H. Shin, et al. Advanced Functional Materials. 2015, 25, 361;
3. F. Wang, D. Liu, J. Li, M. Ma. Advanced Functional Materials. 2018, 1803193;
4. F. Wang, D. Liu, J. Li, M. Ma. ACS Applied Materials & Interfaces. 2017, 9, 37888−37897;
5. K. Klimes, Z. Zhu, J. Li. Advanced Functional Materials. 2019, 29, 1903068.
6. R. Wang, Y. Wang, N. Lin, R. Zhang, et al. Chemistry of Materials. 2018, 30, 8771.
7. M. Hong, M. Ravva, P.Winget, J. Brédas. Chemistry of Materials. 2016, 28, 5791.
8. S. Tasaki, K. Nishimura, H. Toyoshima, T. Masato, et al. SID 2022 DIGEST 506 (ISSN 0097-996X/22/5301-0506-$1.00 © 2022 SID)